

ENDMEMBER VARIABILITY IN HYPERSPECTRAL ANALYSIS

A. Zare, Member, IEEE and K. C. Ho, Fellow, IEEE

1. INTRODUCTION

A wide range of applications including planetary exploration, environmental monitoring, and target detection have been tackled using hyperspectral image analysis. In all of these applications, a prominent area of study is in the development of spectral unmixing and endmember estimation techniques [1]. Endmembers are the *spectral signatures*, the radiance or reflectance values over hundreds of contiguous spectral bands, of the pure, constituent materials in a hyperspectral scene. Given a hyperspectral image, endmember estimation is the task of extracting the spectral signatures for all of the materials located in the scene. Spectral unmixing estimates the proportions of each endmember at every spatial location. In the overwhelming majority of hyperspectral unmixing and endmember estimation algorithms, pixels in a hyperspectral image are modeled as convex combinations of endmembers,

$$\mathbf{x}_n = \sum_{m=1}^M p_{mn} \mathbf{e}_m + \boldsymbol{\epsilon}_n \quad n = 1, \dots, N \quad (1)$$

such that $p_{mn} \geq 0$ and $\sum_{m=1}^M p_{mn} = 1$ and where \mathbf{x}_n is a $D \times 1$ vector containing the spectral signature of the n^{th} pixel in a hyperspectral image, N is the number of pixels in the image, M is the number of endmembers (or materials) found in the scene, p_{mn} is the proportion of endmember m in pixel n , and \mathbf{e}_m is the $D \times 1$ vector containing the spectral signature of the m^{th} endmember, $\boldsymbol{\epsilon}_n$ is an error term, and D is the number of spectral bands (i.e., the dimensionality) of the hyperspectral data [1]. Although used extensively in the literature, the linear mixing model in (1) lacks the ability to represent the spectral variability of the endmembers in a scene. Instead, endmember spectral signatures are represented as single points in a high dimensional space.

The spectral signature for a material varies within hyperspectral data collections due to a number of reasons including environmental, atmospheric, and temporal factors. A material may also have intrinsic spectral variability. One major source of spectral variability results from variation due to illumination conditions [2, 3]. Changes in illumination can result from variation in topography and surface roughness leading to varying levels of shadowed and brightly lit regions. Illumination is also dependent on solar elevation, solar azimuth, and local incidence angle on the material of interest [2]. Differences in the architecture of plant canopies, changes in the distribution of leaf orientation in vegetated regions, or varying building structure and layout in urban areas cause differing il-

lumination levels and areas of shade [4]. When considering minerals, changes in grain size and texture affect illumination. In this case, smaller grain sizes allow for stronger and more uniform backscattered energy resulting in shallower absorption features and higher reflectance values [5]. If accurate digital terrain-elevation models and photometric information are known for an area, then some of the effects of illumination may be able to be removed. However, in general, this information is unavailable for a scene and, if it were known, would require significant computationally-intensive pre-processing.

Another significant source of spectral variation results from changing atmospheric conditions. In particular, the levels of atmospheric gases and aerosols such as water vapor, oxygen, ozone, carbon monoxide and carbon dioxide can absorb and scatter radiation and, thus, cause a significant impact on the measured spectral signature of a material [6]. Many atmospheric gases have strong absorption features or scattering characteristics in a number of wavelengths throughout the electromagnetic spectrum. These absorption and scattering features modify measured spectral signatures as they affect the downward and upward transmittance of radiation from the sun to the surface being measured and, then, from the ground surface to the hyperspectral sensor. In a common spectral radiance model, the downward transmittance of radiation to surface is a combination of the direct solar radiation from the sun to the ground surface; the skylight also known as the *diffuse transmittance* which is the solar radiation that is scattered by atmospheric gases and aerosols and redirected towards the ground surface being measured; and light due to multiple, repeated reflections and scattering from neighboring surfaces and the atmosphere. Then, the total upward transmittance is a combination of the light reflected by the ground surface; light reflected by the ground surface and re-scattered by atmospheric gases and aerosols; and sunlight scattered by the atmosphere and redirected towards the sensor without reaching a ground surface [7]. A number of approaches have been developed that attempt to remove the atmospheric effects from hyperspectral data, however, some of the spectral variability due to atmospheric conditions may not be eliminated using these approaches. For example, as discussed by Gao *et al.* [8], many of these approaches may not accurately account for nitrogen dioxide levels in the atmosphere which can be extremely high in urban areas or measured radiance from a pixel may be modified by the radiance of neighboring pixels due to scattering of solar radiation by atmospheric molecules.

Table 1. Overview of some benefits and challenges to endmember variability representations

	Endmembers as Sets	Endmembers as Statistical Distributions
Advantages	Makes use of a non-parametric representation that does not require the assumption of any particular distribution on spectral values. The approach can be easily constrained to only physically-possible spectral signatures.	Makes use of an efficient, compact, and continuous representation that can account for a range of spectral values that may not have been previously measured for inclusion in a discrete spectral library.
Challenges	Accuracy is limited by the endmember representatives that have been measured or extracted from input data for inclusion during spectral unmixing.	Accuracy of results is dependent on the selection of an accurate parametric form and parameter values. Depending on these selections, this approach may result in representations that allow not physically meaningful endmember variations.
Typical Methods	<p>MESMA, MELSUM, BSMA, & AutoMCU: <i>Pros:</i> Direct and straightforward to apply; <i>Cons:</i> Computationally inefficient.</p> <p>Endmember Bundles: <i>Pros:</i> Designed to quantify proportion indeterminacy; <i>Cons:</i> Accuracy dependent on chosen endmember “seeds.”</p> <p>Band-weighting & Transformation: <i>Pros:</i> Computationally efficient; Maximized between-endmember variance to reduce unmixing confusion <i>Cons:</i> Noise correlation affected after transformation.</p> <p>Sparse & Local Unmixing: <i>Pros:</i> Explicit spectral library not required a priori; Data-point or region specific endmember sets allowed; <i>Cons:</i> Enforcing sparsity and spatial assumptions that may be invalid (e.g., edges).</p>	<p>Bayesian Source Separation: <i>Pros:</i> Joint estimation of end-members and proportions; Endmembers not limited by spectral library; <i>Cons:</i> Full specifications of endmember distributions needed; Physically unrealistic endmembers may be allowed.</p> <p>Normal Compositional Model: <i>Pros:</i> Efficient use of Gaussian distribution; <i>Cons:</i> Physically unrealistic endmembers included; Covariance between bands not addressed.</p> <p>Beta Compositional Model: <i>Pros:</i> Reflectance values constrained to physically-meaningful range; Able to represent skew in endmember distributions; <i>Cons:</i> Detailed specifications of endmember distributions required.</p> <p>Methods of Higher Moments: <i>Pros:</i> Simple form to address any endmember distribution; <i>Cons:</i> Accuracy limited by number of moments used; Endmember moments needed in advance.</p>

Although spectral variability due to these sources is expected, unmixing and endmember estimation methods generally do not account for spectral variability. As such, errors resulting from inaccurate endmember representation will be propagated throughout analysis. The most prominent effects from inaccurate endmember representations are resulting errors in estimated proportion values, termed *proportion indeterminacy*, or the use of too many endmembers to represent a spectrum [4]. In order to avoid these errors and to represent spectral variability during analysis, a number of spectral unmixing and endmember estimation algorithms that incorporate spectral variability have been developed in the literature [9]. As shown by results presented by Garcia-Haro *et al.* [4], accounting for endmember variability can result in a significant improvement in proportion estimation and signal fitting. Previous work by Somers *et al.* [9] has reviewed a number of methods in using the endmembers as sets approach to account for spectral variability. The current paper extends the review for the latest developments of this approach, and includes the other approach of endmembers as statistical distributions which was not discussed in [9]. The objective here is to provide a comprehensive overview of the two approaches with an algorithmic and signal processing viewpoint.

Methods that account for endmember spectral variability can be organized into two general categories based on the variable endmember representation used: endmembers as sets (which can also be seen as a linear mixing model approach) and endmembers as statistical distributions (which can be seen as a stochastic mixing model approach). The for-

mer has a longer history and the latter is more recent. Both of these representations come with associated advantages and challenges; some of these are listed in Table 1. In the following, a review of these methods is provided.

2. ENDMEMBERS AS SETS

One approach to account for spectral variability is to represent each endmember of a material with a set or “bundle” of spectra. Generally speaking, with this representation, a pixel will be modeled as a convex combination of one or more representatives selected from different sets of spectral signatures.

2.1. Known Spectral Library

2.1.1. MESMA, MELSUM, BSMA, & AutoMCU

Several methods for spectral unmixing estimate proportion values by exhaustively searching a given spectral library for endmembers whose corresponding estimated proportion values satisfy some criteria. The most prominent of these approaches is the multiple endmember spectral mixture analysis, MESMA, algorithm [10]. MESMA estimates proportions for an input pixel by searching the endmembers for which proportion values are found that satisfy three conditions: (1) the root mean square (rms) error between the input pixel and its reconstruction using endmembers and proportions is below a prescribed threshold, $rms(\mathbf{x}_n, \{\mathbf{e}_m\}_{m=1}^M) < t$, where,

$$rms(\mathbf{x}_n, \{\mathbf{e}_m\}_{m=1}^M) = \min_{p_{mn}} \left(\sqrt{\frac{1}{D} \left\| \mathbf{x}_n - \sum_{m=1}^M p_{mn} \mathbf{e}_m \right\|_2^2} \right) \quad (2)$$

and $\{\mathbf{e}_m\}_{m=1}^M$ is the collection of M endmembers used to unmix the pixel; (2) the rms error for contiguous spectral bands is below a prescribed threshold; and (3) the estimated proportion values are within some prescribed range. This range may be fixed to $[0 \leq p_{mn} \leq 1]$ or, to account for some error in endmember or proportion values allow for values slightly outside of this range (e.g., $[-0.01 \leq p_{mn} \leq 1.01]$). This approach allows each input pixel from a hyperspectral scene to be represented using a unique collection of endmember spectra from the spectral library. Therefore, even if each input pixel is restricted to be represented by, for example, no more than three endmembers, the full scene can be mapped using many more.

When the spectral library is large, there will be a considerable number of elements to choose from. In such a case, MESMA may result in difficulties such as finding an overabundance of viable solutions or extreme computational inefficiency by exhaustively searching over all possible combinations of endmembers. A number of extensions to MESMA attempt to mitigate these difficulties such as defining methods for pruning endmembers before applying MESMA.

There are a number of variants based on MESMA. The Multiple-Endmember Linear Spectral Unmixing (MELSUM) method relaxes the criteria to identify viable proportions where non-negative values are sufficient [5]. The Bayesian Spectral Mixture Analysis (BSMA) method obtains the final proportion value of a material in a pixel through a weighted sum of the proportion values found in all combinations, where the weights are proportional to the probabilities of each endmember deduced from the spectral library [11]. The Automated Monte Carlo Unmixing (AutoMCU) method randomly selects endmembers from the spectral library to unmix the hyperspectral scene over several times [12], rather than doing exhaustive search. The proportion values of each pixel are summarized using their mean and standard deviation associated with each material from the several runs. In addition to improving computational efficiency, AutoMCU is able to quantify explicitly the proportion indeterminacy.

MESMA, MELSUM, BSMA, and AutoMCU do not inherently address spectral variability without an appropriate spectral library. The spectral library must have more than one spectra to represent each material and they are grouped together to form the set E_m , $m = 1, 2, \dots, M$, where M is the number of materials. Then, during unmixing, one or none of the spectra from each set are selected to estimate proportion values, i.e., $\mathbf{e}_m \in E_m$. As such, when an appropriate spectral library is provided, each pixel can be unmixed using a unique spectral variation of each material.

During unmixing, these approaches often also account for variability due to illumination by including a “shade” endmember [3]. The shade effect often corresponds to multiplication factor in the hyperspectral image. In the linear mixing model, however, the shade effect can be accounted for through normalization of the image data or the addition of a

photometric shade endmember (i.e., the origin) because they are mathematically equivalent.

2.1.2. Endmember Bundles

The Endmember Bundles unmixing approach was designed to explicitly address spectral variability and quantify the associated proportion indeterminacy [13]. It estimates the minimum and maximum proportion values for the m^{th} material of pixel \mathbf{x}_n by minimizing (3) and (4), respectively,

$$p_{min,mn} = \min_{p_{1n}, \dots, p_{Tn}, s} \sum_{i=1}^T \chi_{m,i} p_{in} + ws \quad (3)$$

$$p_{max,mn} = \max_{p_{1n}, \dots, p_{Tn}, s} 1 - \left[\sum_{i=1}^T (1 - \chi_{m,i}) p_{in} + ws \right] \quad (4)$$

where

$$\chi_{m,i} = \begin{cases} 1 & \text{if } \mathbf{e}_i \in E_m; \\ 0 & \text{if } \mathbf{e}_i \notin E_m. \end{cases} \quad (5)$$

The minimization is over the non-negative proportion values p_{in} that must satisfy $\mathbf{x}_n = \sum_{i=1}^T p_{in} \mathbf{e}_i + s\mathbf{d}$ and $\sum_{i=1}^T p_{in} = 1$. T is the total number of elements across all endmember sets, \mathbf{e}_i denotes the i^{th} spectral signature across the whole library, E_m is the endmember set composed of all endmember spectra of the m^{th} material, and $\mathbf{d} = \mathbf{x}_n - \frac{1}{T} \sum_{i=1}^T \mathbf{e}_i$. The variables $s \in [0, \infty)$ and $w \in [0, \infty)$ are used to minimize the residual error. The parameter w is set to a very large value (tending towards ∞) to drive the estimated s value towards zero. The optimization is conducted using Dikin’s affine algorithm method [13]. Given these min and max proportion values, the mean proportion value can also be computed, $p_{mean,mn} = (p_{min,mn} + p_{max,mn})/2$.

2.1.3. Band Selection, Weighting and Transformation

Another approach to address spectral variability is through band selection or weighting [9] such that the wavelengths with minimum spectral variability are the ones that are primarily used for spectral unmixing. Extending this concept, one could find spectral transformations that transform the input hyperspectral data into a space that minimizes the effect of spectral variability. In particular, the Fisher Discriminant approach (FDA) for spectral unmixing learns a transformation for the spectral signature elements in order to minimize the scatter within endmember sets and maximize the scatter among them prior to the estimation of proportion values [14] to avoid unmixing confusion [15]. The goal of FDA is to estimate the transformation projection matrix, $\widehat{\mathbf{W}}$,

$$\widehat{\mathbf{W}} = \arg \max_{\mathbf{W}} \frac{|\mathbf{W}^T \mathbf{S}_b \mathbf{W}|}{|\mathbf{W}^T \mathbf{S}_w \mathbf{W}|} \quad (6)$$

where \mathbf{S}_b and \mathbf{S}_w are between- and within-class dispersion matrices [16]. Each pixel is transformed by $\widehat{\mathbf{W}}$ before estimating proportion values and (1) becomes

$$\widehat{\mathbf{W}} \mathbf{x}_n = \sum_{m=1}^M p_{mn} \widehat{\mathbf{W}} \mathbf{e}_m + \widehat{\mathbf{W}} \mathbf{\epsilon}_n \quad n = 1, \dots, N. \quad (7)$$

An effective transformation matrix will make the transformed elements within the same set nearly identical to each other and, thus, any one of the transformed elements from each of the endmember sets can be used to estimate the corresponding proportion values for that material. This linear transformation will affect the noise distribution and, to address this, the noise correlation can be accounted for through the use of a weighting matrix when estimating the proportion values.

2.1.4. SVM Unmixing

A number of approaches using support vector machines (SVM) have been developed for spectral unmixing while addressing spectral variability [17, 18]. SVM is a commonly used supervised two-class classifier. Given a training set, $\{(\mathbf{x}_1, y_1), (\mathbf{x}_2, y_2), \dots, (\mathbf{x}_N, y_N)\}$ where \mathbf{x}_i is the i^{th} data point and $y_i \in \{0, 1\}$ is the desired class label, SVM learns a hyperplane that separates the two classes [16]. In the context of hyperspectral unmixing, the two SVM classes are the favorable class containing pixels from mixing endmembers at specific proportion values vs the unfavorable class of those coming from other proportion choices. To elaborate further [17], the first step for SVM unmixing is to discretize the solution space of unmixed proportions to a finite number of candidates. For example, if two materials are under consideration, with a proportion resolution of 0.1 for each material, nine proportion solution candidates $[(.9, .1), (.8, .2), \dots, (.1, .9)]$ are generated. For each candidate, synthesized pixel data are created by drawing elements from the endmember sets and mixing them according to the proportion candidate. Next, a number of SVMs are trained, one for each solution candidate, by labeling the synthesized data of the selected candidate as 1 and the rest as 0. Given an unknown pixel for unmixing, it is evaluated through all of the SVM classifiers and the SVM that gives the largest classification margin will identify the corresponding candidate as the unmixed proportion solution.

One advantage of SVM unmixing is that spectral variability is automatically taken care when creating synthesized data for SVM training. Due to the discretization of proportion values, however, this approach produces a finite and possibly limited number of abundance proportion choices only, which might be not acceptable in some applications.

2.2. Unknown Spectral Library

Spectral libraries can be obtained using laboratory measurements of materials of interest or manual endmember identification from the imagery under study or data previously acquired. Often, spectral libraries or the expertise needed to identify spectral signatures of various materials is unavailable. Thus, approaches to autonomously estimate endmember sets and perform spectral unmixing of input data are needed.

2.2.1. Automated Endmember Bundles

Earlier work [13] proposes a semi-automatic endmember set estimation technique. It begins with manually selected “endmember seeds” and grows an endmember set by identifying

the data pixels that have high correlation coefficients with the seeds, provided that spectral reflectance values are constrained to the physically-meaningful range of 0 to 1.

In the subsequent work [19], Somers *et al.* developed a fully automated approach for building endmember sets by repeatedly applying a standard endmember extraction method, such as Vertex Component Analysis (VCA) [20], to a randomly selected portion of the input data. The endmember sets are obtained by grouping all of the estimated endmembers into M clusters using the K -means clustering algorithm. After extracting the endmember sets, any of the previously described spectral unmixing methods can be applied.

2.2.2. Sparse Unmixing

The Automated Endmember Bundles technique treats endmember set estimation independently from proportion estimation in unmixing. However, many endmember estimation approaches are paired with spectral unmixing steps such as with most sparse unmixing approaches. Various sparsity approaches can also be categorized in terms of the specific sparsity constraint employed such as l_0 norm constraints or inclusion of l_1 regularization terms. In the sparse unmixing approach for endmember variability presented by Castrodad *et al.* [21], endmember set estimation is conducted in conjunction with unmixing on a training dataset containing many examples of a material. In particular, given N_m pixels composed purely of material m that is denoted by the $D \times N_m$ matrix \mathbf{X}_m , the dictionary elements representing the endmember set of material m , represented by the columns of the matrix $\tilde{\mathbf{E}}_m$, are obtained by minimizing the objective function,

$$R(\tilde{\mathbf{E}}_m, \mathbf{P}_m) = \left\| \mathbf{X}_m - \tilde{\mathbf{E}}_m \mathbf{P}_m \right\|_F^2 + \lambda_S \|\mathbf{P}_m \mathbf{1}\|_1 \quad (8)$$

where each column of \mathbf{P}_m represents the proportion values contributed from different columns of $\tilde{\mathbf{E}}_m$, $\mathbf{1}$ is a length N_m column vector of unity and λ_S is a fixed regularization parameter. The N_m pixels in \mathbf{X}_m are given from some training data such as hand-selected from a ground-truthed data set. The second term in the objective function promotes more sparseness as λ_s increases. The function is minimized through alternating optimization by solving for updated $\tilde{\mathbf{E}}_m$ and \mathbf{P}_m values, iteratively. After minimization of (8), the endmember set of material m is constructed by maintaining the columns in $\tilde{\mathbf{E}}_m$ that are being used to describe the training set, $E_m = \left\{ \tilde{\mathbf{e}}_j : j \ni \sum_{n=1}^{N_m} p_{jn} > 0 \right\}$ where \ni denotes “such that”, p_{jn} is the (j, n) element of \mathbf{P}_m . The minimization is conducted using a Gauss-Seidel type iteration as discussed in [21].

After the dictionary elements are obtained, spectral unmixing can be conducted on previously unseen hyperspectral data \mathbf{x}_n . Let \mathbf{E}_m be the $D \times |E_m|$ matrix whose columns are the elements of the dictionary E_m obtained above and where $|E_m|$ is the number of elements in the m^{th} dictionary. Also, let \mathbf{p}_{mn} be a $|E_m| \times 1$ vector that represents the proportion values of the elements in E_m . The unmixing is achieved

through the minimization of the following objective,

$$\begin{aligned} & \left\| \mathbf{x}_n - \sum_{m=1}^M \mathbf{E}_m \mathbf{p}_{mn} \right\|_2^2 + \lambda_S \sum_{m=1}^M \|\mathbf{p}_{mn}\|_1 \\ & + \lambda_G \sum_{m=1}^M \left\| \mathbf{p}_{mn} - \sum_{i \in \mathcal{R}(n)} w_{ni} \mathbf{p}_{mi} \right\|_2^2 \end{aligned} \quad (9)$$

where $\mathcal{R}(n)$ is the neighborhood defined around the n^{th} data point, $w_{ni} = \frac{1}{Z_i} \exp \left\{ -\|\mathbf{x}_n - \mathbf{x}_i\|_2^2 / \sigma^2 \right\}$, Z_i is a pixel-dependent normalization constant such that $\sum_i w_{ni} = 1$, σ^2 is a fixed constant and λ_G is a fixed regularization parameter. The second term in the objective function promotes sparsity. The third term can be viewed as a spatial smoothing term in which pixels in the same neighborhood are encouraged to have similar proportion values. Increasing σ^2 enlarges the neighborhood region and larger λ_G enhances spatial smoothing more.

2.2.3. Local Unmixing

Local unmixing extracts endmember sets with elements identified in spatial neighborhoods across the input hyperspectral image [22, 23]. In the technique developed by Goenaga *et al.* [23], an input hyperspectral image is divided into equally-sized tiles. Local endmembers are extracted manually or using some endmember extraction method. The extracted local endmembers are clustered using spectral angle criteria to form the endmember sets. Proportion values are obtained

by minimizing $\left\| \mathbf{x}_n - \sum_{i=1}^T p_{in} \mathbf{e}_i \right\|_2^2$ subject to $p_{in} > 0$ and $\sum_i p_{in} \leq 1$. The proportion of a material is computed by the sum of the proportion values associated with its clustered elements, $p_{mn} = \sum_{j \ni \mathbf{e}_j \in E_m} p_{jn}$.

One interesting point of discussion is that local unmixing approaches assume pixels that are spatially-close are likely to be composed of the same materials. This assumption could be viewed as a balance between (a) the traditional hyperspectral unmixing algorithms that consider all pixels in a scene to be composed of the same endmember elements and (b) the pixel to pixel independent spectral variability approaches such as MESMA, AutoMCU, and MELSUM where every input pixel in a scene could be composed of a completely unique collection of elements from across the endmember sets.

Sparse unmixing applied to a dictionary consisting of several variants of each endmember can be used to address spectral variability. In terms of local unmixing, we can impose neighboring pixels with the same dictionary elements in their sparse representation. In the spectral-variability sparse unmixing approach presented above, in addition to the sparsity constraint, pixels in pre-defined neighborhoods are encouraged to be composed of the same materials at roughly the same proportion levels. The pre-defined neighborhoods are not restricted to spatial neighborhoods and could be neighborhoods based spectral similarity. Similar ideas have been ap-

plied using the piece-wise convex unmixing methods, which identify groups of pixels (not necessarily spatial neighbors) that are constrained to have same endmember elements during unmixing [24].

These additional constraints based on spatial or spectral neighborhoods impose additional structures that further confine the solution space during spectral unmixing. However, the applicability of each of these additional constraints is certainly data- and application-dependent.

3. ENDMEMBERS AS DISTRIBUTIONS

An alternative to the set-based approach to address spectral variability in a material is the use of a multi-variate statistical distribution. When endmembers are represented as statistical distributions, then, a sample from these distributions can be viewed as a possible variation on the spectral signature of the material being represented,

$$\mathbf{e}_m \sim \mathcal{F}(\cdot | \boldsymbol{\theta}_m) \quad (10)$$

where \mathcal{F} is the multi-variate statistical distribution used to represent an endmember and $\boldsymbol{\theta}_m$ are parameters of the distribution associated with the m^{th} material. Under this approach, hyperspectral pixels are random variables distributed according to the stochastic mixture model defined by the convex combination of the endmembers, $\mathbf{x}_n = \sum_{m=1}^M p_{mn} \mathbf{e}_m$ where \mathbf{e}_m is a random variable distributed according to $\mathcal{F}(\mathbf{e}_m | \boldsymbol{\theta}_m)$. There is no additive noise in this model as variation in the \mathbf{x} value are accounted for through the stochastic model and the variability of the endmember distributions.

A number of methods make use of a Bayesian approach for endmember estimation and spectral unmixing. When the distributions of the endmembers are completely specified, joint estimation of endmembers and proportions, such as Bayesian source separation and non-negative matrix factorization, can also provide endmember variations in spectral unmixing [25, 26]. In particular, [25], assumes a Gamma distribution as the prior for each value of the endmembers. Such an approach requires exact knowledge of the endmember distributions which may not be easy to obtain in practice. In the Normal Compositional Model (NCM) methods described below, the models imposed on the endmember distributions do not require complete specification and the unknown distribution parameters are jointly estimated together with proportions during unmixing.

3.1. Normal Compositional Model

By far the most prominent statistical distribution for endmembers is the NCM [27] and as a result,

$$\mathbf{x}_n \sim \mathcal{N} \left(\cdot \left| \sum_m^M p_{mn} \boldsymbol{\mu}_m, \sum_m^M p_{mn}^2 \boldsymbol{\Sigma}_m \right. \right) \quad (11)$$

in which $\mathcal{F}(\mathbf{e}_m | \boldsymbol{\theta}_m) = \mathcal{N}(\mathbf{e}_m | \boldsymbol{\mu}_m, \boldsymbol{\Sigma}_m)$ where $\boldsymbol{\mu}_m$ are endmember mean values and $\boldsymbol{\Sigma}_m$ are the endmember covariances. A number of methods for spectral unmixing and endmember estimation have been developed using the NCM.

Stein [27] proposed an Expectation-Maximization algorithm to iteratively update proportion values for every input pixel as well as the mean and variance parameter values for each endmember distribution using the NCM, until convergence is reached.

Under the condition that the mean values of the endmembers are known, Eches *et al.* [28] develop a Markov Chain Monte Carlo (MCMC) sampling approach for estimating proportion values and the endmember distribution covariance using the NCM. The hierarchical Bayesian framework is,

$$\mathbf{x}_n | \mathbf{p}_n, \sigma^2 \sim \mathcal{N} \left(\cdot \left| \sum_{m=1}^M p_{mn} \boldsymbol{\mu}_m, \sum_{m=1}^M p_{mn}^2 \sigma^2 \mathbf{I} \right. \right) \quad (12)$$

$$\mathbf{p}_n \sim \mathcal{D}(\cdot | \mathbf{1}) \quad (13)$$

$$\sigma^2 | \delta \sim \mathcal{IG}(\cdot | \nu, \delta) \quad (14)$$

where $\mathcal{D}(\cdot | \mathbf{1})$ is Dirichlet distribution such that all parameter values are equal to 1 (i.e., a uniform distribution over the set of proportion values that satisfy the non-negativity and sum-to-one constraints), $\mathcal{IG}(\nu, \delta)$ is an inverse-gamma distribution with parameter values ν and δ in which, for the implementation presented in [28], $\nu = 1$ and δ is assigned a given non-informative Jeffreys prior, and \mathbf{I} is the identity matrix. To estimate the unknown proportion $\mathbf{p}_n = [p_{1n}, p_{2n}, \dots, p_{Mn}]^T, \forall n = 1, \dots, N$, the endmember variance σ^2 and the parameter δ , a Metropolis-within-Gibbs sampler is used. In [28], endmember covariances are assumed to be diagonal and may not be identical.

Zare *et al.* [24] also develop an MCMC sampling approach under the NCM. However, in contrast to the method by Eches *et al.*, it assumes endmember covariance values are available and the endmember means and proportion values are to be estimated. The hierarchical Bayesian framework defined for a single set of endmember distributions is,

$$\mathbf{x}_n | \Pi, \mathbf{p}_n \sim \mathcal{N} \left(\cdot \left| \sum_{m=1}^M p_{mn} \boldsymbol{\mu}_m, \sum_{m=1}^M p_{mn}^2 \boldsymbol{\Sigma}_m \right. \right) \quad (15)$$

$$\boldsymbol{\mu}_m \sim \mathcal{N}(\cdot | \mathbf{m}, \mathbf{C}) \quad (16)$$

$$\mathbf{p}_n \sim \mathcal{D}(\cdot | \mathbf{1}) \quad (17)$$

where $\Pi = [\boldsymbol{\mu}_1, \boldsymbol{\mu}_2, \dots, \boldsymbol{\mu}_M]$ is the collection of endmember means, $\mathbf{p}_n = [p_{1n}, p_{2n}, \dots, p_{Mn}]^T$ is the vector of proportion values, \mathbf{m} and \mathbf{C} are hyperparameters defining the prior distribution on the endmember means. The \mathbf{m} and \mathbf{C} values are parameters to be fixed (such as setting them to the mean and covariance data). In [24], additional hyper-priors are applied to \mathbf{m} and \mathbf{C} such that $\mathbf{m} \sim \mathcal{N}(\cdot | \frac{1}{N} \sum_{n=1}^N \mathbf{x}_n, \mathbf{V})$ and $\mathbf{C} \sim IW(\Psi, t)$ to allow for multiple sets of endmember distributions in a piece-wise convex mixing model. Using the piece-wise convex approach, input data pixels are partitioned into sets that are composed of mixtures of the same materials. The partitions are estimated by incorporating a Dirichlet Process prior from

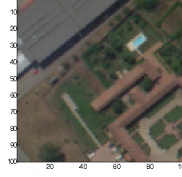


Fig. 1. RGB image (bands 56, 29, 12) of the Pavia sub-scene.

which partitions of the input data set are sampled. To estimate the endmember means and proportion values, a Metropolis-within-Gibbs sampler is proposed.

3.2. Beta Compositional Model

The majority of investigation with endmembers as distributions has been conducted using the NCM. Yet, investigation into alternative compositional models, such as the Beta Compositional Model (BCM) has been conducted [29]. Under the BCM, the input data points are random variables distributed according to a convex combination of Beta random variables. The motivation for the use of the Beta is that the values are constrained to the range from zero to one which is appropriate and a physically-meaningful range for endmember reflectance values. The spectral unmixing method developed in [29] based on the BCM assumes known endmember parameter values and estimates proportion values for input pixels using an approximation to the BCM.

3.3. Methods of Higher Moments

In the approach presented by Bosdogianni *et al.* [30] rather than defining a fixed parametric form for each endmember distribution, given known values for the first and second moments of each endmember distribution, proportion values of an input data set are estimated by minimizing the squared difference between the first and second moments of the estimated convex combination of the endmember values and those of the input data. Given that statistics of the full input data set are used to estimate proportion values, pixel-specific proportion values are not estimated but, instead, test-site wide values. An advantage to this approach is that the full parametric form for each endmember distribution does not need to be specified and, instead, only the first and second moments (equivalent to mean and covariance) of each endmember distribution are needed. Using only the first two moments follows a symmetric distribution as in the NCM. However, presumably, this approach could be extended to include higher order moments.

4. RESULTS

A sampling of five methods, one from typical unmixing method without accounting for spectral variability, and two from each representation of spectral variability are used: (1) VCA+FCLS, (2) the Automated Endmember Bundles (AEB) by Somers *et al.* [19], (3) the Local Unmixing (LU) approach by Goenaga *et al.* [23], (4) the NCM approach by Eches *et al.* [28] NCM-1, and (5) the NCM approach by Zare *et al.* [24]

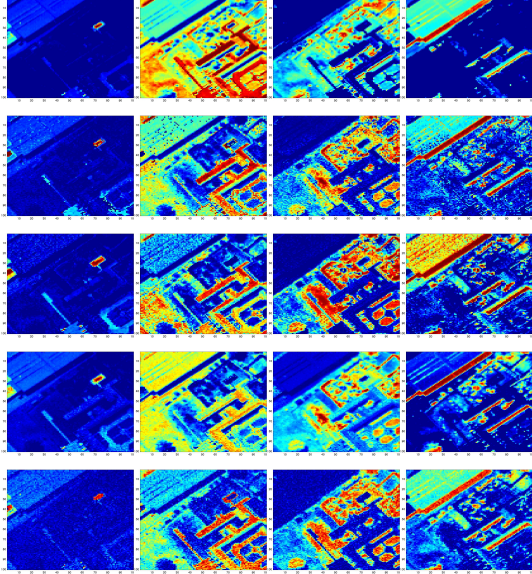


Fig. 2. Proportion maps of the Pavia sub-image from VCA + FCLS (row 1); Automated Endmember Bundles (row 2); Local Unmixing (row 3); NCM [28]: (row 4); NCM [24]: (row 5); of water, buildings & dirt, vegetation, and shadow.

NCM-2. These algorithms were applied to a 100×100 pixel sub-image collected by the Reflective Optics System Imaging Spectrometer (ROSIS) over an urban area of Pavia in northern Italy on July 8, 2002. The RGB image of the scene is in Figure 1. The image contains spectra from vegetation and man-made objects.

All the methods were set with four endmember sets or distributions ($M=4$). Note that the performance could vary when different value of M is used, too large M splits a material across multiple proportion values and too small M groups distinct materials. The results are shown in Figure 2.

Each of these methods requires a number of parameter settings that are encumbered with various tradeoffs between running time and accuracy. In VCA+FCLS, VCA is used for endmember extraction and Fully Constrained Least-Squares (FCLS) [31] is applied for proportion estimation. It does not assume spectral variability and is served as a reference for comparison. The AEB estimated the four endmember sets by repeatedly applying the VCA algorithm with 3000 iterations to 5000 randomly-sampled pixels from the scene. The proportion values were obtained using MESMA [19]. LU obtained endmembers on 33×33 -sized tiles across the image using VCA [20]. After which, the resulting local endmembers were clustered into four endmember sets from which proportion values were estimated [23]. NCM-1 generated the means of the four endmembers using VCA and per-pixel proportion values were estimated using 1000 iterations of MCMC sampling. NCM-2 used iso-tropic diagonal covariance matrices with values of 0.01 and the corresponding MCMC sampling algorithm was iterated 200 times.

The results are shown in Figure 2. As a measure of improvement in spectral unmixing, we used two approaches: (1) the average per-pixel squared residual (signal fitting) error for each pixel and (2) the median of the proportion maps over the five methods as an ideal output to compute the residual unmixing error. The average squared residual error were as follows: VCA+FCLS: 0.403, AEB: 0.009, LU: 0.010, NCM-1: 0.191, NCM-2: 0.108. The percentage in mean-square residual errors of the five methods were: VCA+FCLS: 32.3%, AEB: 5.9%, LU: 9.1%, NCM-1: 10.6%, NCM-2: 5.2%. The performance of the four methods with spectral variability is consistent and the amount of error reduction over VCA+FCLS is significant. Obviously, the cost of better results from spectral variability unmixing is the increase in computation time, which is proportional to the number of endmembers M . In general, endmembers as distributions approach could have computational advantage over endmembers as sets if the endmember sets are large.

5. SUMMARY AND FUTURE WORK

This paper presented an overview of methods that address spectral variability for hyperspectral unmixing and end-member estimation. Although significant progress has been made in this area, there are several open lines of research. In particular, as discussed above, many of the current approaches rely on the availability of known spectral libraries and results are highly dependent on the availability of appropriate end-member spectra. Given an extremely large spectral library, investigation into automated pruning and sub-selection of the library for maintaining scene-appropriate endmembers is needed. The applicability of these libraries depends upon items such as the inclusion of the materials found in the scene with the exclusion of spectrally-similar confusers.

Automated parameter setting for all of these approaches is another subject for study. In particular, appropriate selection of the number of endmembers can have a large impact on the quality of results. Many of the existing methods rely on manual selection through trial-and-error or broad assumptions (i.e., a fewer number of endmembers is better).

Additional investigation of methods to leverage spatial information can be conducted. Methods employed in the image processing and computer vision communities make extensive use of color and texture information for scene understanding. An area of study is in how these or similar approaches can be transferred to hyperspectral image analysis. The challenge is the being able to effectively balance spatial information without loss of the sub-pixel information.

In addition to linear mixing model as in (1), non-linear mixing (such as bi-linear model [1]) can be used to account for different phenomena such as multiple reflections or intimate mixtures of materials, resulting in more accurate endmember and proportion estimates. Interesting future work will include incorporating spectral variability into non-linear mixing models and identifying when non-linear or linear

models with or without spectral variability are needed.

Additionally, future investigation into models that limit variability to physically-meaningful values should be conducted. Also, all of the current methods in this area assume independent variation between the bands of an endmember. In practice, neighboring bands are often highly correlated and extension of these models to make use of full covariances to account for this correlation is needed. In addition, these models are currently limited to representing all endmembers with distributions of the same parametric form. It is possible that differing materials may be best represented with different forms. The extension of these approaches to mixed-form models is an interesting subject for investigation.

Finally, future work remains in developing evaluation metrics or measured data sets with proportion-level ground-truth to allow for evaluation of methods which address spectral variability. An open problem remains in how to determine whether a particular spectrum is a variation on an endmember or a mixed pixel with high abundance of an endmember.

- [1] J. Bioucas-Dias, A. Plaza, N. Dobigeon, M. Parente, Q. Du, P. Gader, and J. Chanussot, "Hyperspectral unmixing overview: Geometrical, statistical, and sparse regression-based approaches," *IEEE J. Sel. Topics Appl. Earth Observ.*, vol. 5, no. 2, pp. 354–379, Apr. 2012.
- [2] J. Adams, D. Sabol, V. Kapos, R. Filho, D. Roberts, M. Smith, and A. Gillespie, "Classification of multispectral images based on fractions of endmembers: Application to land-cover change in the brazilian amazon," *Remote Sensing of Env.*, vol. 52, no. 2, pp. 137 – 154, May 1995.
- [3] P. Dennison, K. Halligan, and D. Roberts, "A comparison of error metrics and constraints for multiple endmember spectral mixture analysis and spectral angle mapper," *Remote Sensing of Env.*, vol. 93, pp. 359–367, Nov. 2004.
- [4] F. Garcia-Haro, S. Sommer, and T. Kemper, "A new tool for variable multiple endmember spectral mixture analysis (vmesma)," *Int. J. of Remote Sensing*, vol. 26, no. 10, pp. 2135–2162, May 2005.
- [5] J.-Ph. Combe, S. Le Mouelic, C. Sotin, A. Gendrin, J. F. Mustard, L. Le Deit, P. Launeau, J.-P. Bibring, B. Gondet, Y. Langevin, and P. Pinet, "Analysis of omega/mars express data hyperspectral data using a multiple-endmember linear spectral unmixing model (melsum): Methodology and first results," *Planetary and Space Sci.*, vol. 56, pp. 951–978, Dec. 2008.
- [6] G. Healey and D. Slater, "Models and methods for automated material identification in hyperspectral imagery acquired under unknown illumination and atmospheric conditions," *IEEE Trans. Geosci. Remote Sens.*, vol. 37, no. 6, pp. 2706–2717, Nov. 1999.
- [7] J. Nascimento and J. Bioucas-Dias, "Does independent component analysis play a role in unmixing hyperspectral data?," *IEEE Trans. Geosci. Remote Sens.*, vol. 43, no. 1, pp. 175–187, Jan. 2005.
- [8] B. Gao, M. Montes, C. Davis, and A. Goetz, "Atmospheric correction algorithms for hyperspectral remote sensing data of land and ocean," *Remote Sensing of Env.*, vol. 113, Supp. 1, pp. S17 – S24, Sep. 2009.
- [9] B. Somers, G. P. Asner, L. Tits, and P. Coppin, "Endmember variability in spectral mixture analysis: A review," *Remote Sensing of Env.*, vol. 115, no. 7, pp. 1603–1616, Jul. 2011.
- [10] D. Roberts, M. Gardner, R. Church, S. Ustin, G. Scheer, and R. O. Green, "Mapping chaparral in the santa monica mountains using multiple endmember spectral mixture models," *Remote Sensing of Env.*, vol. 65, pp. 267–279, Sep. 1998.
- [11] C. Song, "Spectral mixture analysis for subpixel vegetation fractions in the urban environment: How to incorporate endmember variability?," *Remote Sensing of Env.*, vol. 95, no. 2, pp. 248–263, Mar. 2005.
- [12] G. Asner, M. Bustamante, and A. Townsend, "Scale dependence of biophysical structure in deforested areas bordering the tapajs national forest, central amazon," *Remote Sensing of Env.*, vol. 87, pp. 507–520, Mar. 2003.
- [13] C. A. Bateson, G. P. Asner, and C. A. Wessman, "Endmember bundles: A new approach to incorporating endmember variability into spectral mixture analysis," *IEEE Trans. Geosci. Remote Sens.*, vol. 38, no. 2, pp. 1083–1093, Mar. 2000.
- [14] J. Jin, B. Wang, and L. Zhang, "A novel approach based on fisher discriminant null space for decomposition of mixed pixels in hyperspectral imagery," *IEEE Geosci. Remote Sens. Lett.*, vol. 7, no. 4, pp. 699–703, Oct. 2010.
- [15] P. Dennison and D. Roberts, "Multiple endmember spectral mixture analysis using endmember average rsme," *Remote Sensing of Env.*, vol. 87, no. 2-3, pp. 123–135, Oct. 2003.
- [16] C. Bishop, *Pattern Recognition and Machine Learning*, Springer-Verlag New York, Inc., Secaucus, NJ, USA, 2006.
- [17] F. Mianji and Y. Zhang, "Svm-based unmixing-to-classification conversion for hyperspectral abundance quantification," *IEEE Trans. Geosci. Remote Sens.*, vol. 49, no. 11, pp. 4318–4327, Nov. 2011.
- [18] F. Bovolo, L. Bruzzone, and L. Carlin, "A novel technique for subpixel image classification based on support vector machine," *IEEE Trans. Image Process.*, vol. 19, no. 11, pp. 2983–2999, Nov. 2010.
- [19] B. Somers, M. Zortea, A. Plaza, and G. Asner, "Automated extraction of image-based endmember bundles for improved spectral unmixing," *IEEE J. Sel. Topics Appl. Earth Observ.*, vol. 5, no. 2, pp. 396–408, Apr. 2012.
- [20] J. Nascimento and J. Bioucas-Dias, "Vertex component analysis: a fast algorithm to unmix hyperspectral data," *IEEE Trans. Geosci. Remote Sens.*, vol. 43, no. 4, pp. 898–910, Apr. 2005.
- [21] A. Castrodad, Z. Xing, J. Greer, E. Bosch, L. Carin, and G. Sapiro, "Learning discriminative sparse representations for modeling, source separation, and mapping of hyperspectral imagery," *IEEE Trans. Geosci. Remote Sens.*, vol. 49, no. 11, pp. 4263–4281, Nov. 2011.
- [22] K. Canham, A. Schlamm, A. Ziemann, B. Basener, and D. Messinger, "Spatially adaptive hyperspectral unmixing," *IEEE Trans. Geosci. Remote Sens.*, vol. 49, no. 11, pp. 4248–4262, Nov. 2011.
- [23] M. Goenaga, M. Torres-Madroneiro, M. Velez-Reyes, S. Van Bloem, and J. Chinea, "Unmixing analysis of a time series of hyperion images over the gunica dry forest in puerto rico," *IEEE J. Sel. Topics Appl. Earth Observ.*, vol. 6, no. 2, pp. 329–338, Apr. 2013.
- [24] A. Zare, P. Gader, and G. Casella, "Sampling piecewise convex unmixing and endmember extraction," *IEEE Trans. Geosci. Remote Sens.*, vol. 51, no. 3, pp. 1655–1665, Mar. 2013.
- [25] S. Moussaoui, D. Brie, A. Mohammad-Djafari, and C. Carteret, "Separation of non-negative mixture of non-negative sources using a bayesian approach and mcmc sampling," *IEEE Trans. Signal Process.*, vol. 54, no. 11, pp. 4133–4145, Nov. 2006.
- [26] N. Dobigeon, S. Moussaoui, M. Coulon, J.-Y. Tourneret, and A. O. Hero, "Joint bayesian endmember extraction and linear unmixing for hyperspectral imagery," *IEEE Trans. Sig. Process.*, vol. 57, no. 11, pp. 4355–4368, Nov. 2009.
- [27] D. Stein, "Application of the normal compositional model to the analysis of hyperspectral imagery," in *Proc. of the IEEE Wkshp. on Advances in Techniques for Anal. of Rmtly. Sensed Data*, 2003, Oct. 2003, pp. 44–51.
- [28] O. Eches, N. Dobigeon, C. Mailhes, and J. Y Tourneret, "Bayesian estimation of linear mixtures using the normal compositional model. application to hyperspectral imagery," *IEEE Trans. Image Process.*, vol. 19, no. 6, pp. 1403–1413, Jun. 2010.
- [29] A. Zare, P. Gader and D. Dranishnikov, and T. Glenn, "Spectral unmixing using the beta compositional model," in *Proc. of the IEEE Wkshp. on Hyper. Img. and Sig. Proc.: Evolution in Rmt. Sens.* Jun. 2013.
- [30] P. Bosdogianni, M. Petrou, and J. Kittler, "Mixture models with higher order moments," *IEEE Trans. Geosci. Remote Sens.*, vol. 35, no. 2, pp. 341–353, Mar. 1997.
- [31] D. Heinz and C.-I. Chang, "Fully constrained least squares linear mixture analysis for material quantification in hyperspectral imagery," *IEEE Trans. Geosci. Remote Sens.*, vol. 39, pp. 529–545, Mar. 2001.

Alina Zare (zarea@missouri.edu) is an Assistant Professor in the Electrical and Computer Engineering Department, University of Missouri. Her research interests include machine learning, Bayesian methods, SONAR analysis, image analysis and hyperspectral image analysis.

K. C. Ho (hod@missouri.edu) is a Professor in the ECE Department of the University of Missouri. His research interests are in sensor array processing, source localization and remote sensing. He is a Fellow of the IEEE.